Titre: Title:	Rheological and foaming behavior of linear and branched polylactides
Auteurs: Authors:	Naqi Najafi Chaloupli, Marie-Claude Heuzey, Pierre Carreau, Daniel Therriault, & Chul B. Park
Date:	2014
Type:	Article de revue / Article
Référence: Citation:	Najafi Chaloupli, N., Heuzey, M.-C., Carreau, P., Therriault, D., & Park, C. B. (2014). Rheological and foaming behavior of linear and branched polylactides. Rheologica Acta, 53(10-11), 779-790. https://doi.org/10.1007/s00397-014-0801-3

Document en libre accès dans PolyPublie
Open Access document in PolyPublie

URL de PolyPublie: PolyPublie URL:	https://publications.polymtl.ca/10410/
Version:	Version finale avant publication / Accepted version Révisé par les pairs / Refereed
Conditions d'utilisation: Terms of Use:	Tous droits réservés / All rights reserved

Document publié chez l'éditeur officiel
Document issued by the official publisher

Titre de la revue: Journal Title:	Rheologica Acta (vol. 53, no. 10-11)
Maison d'édition: Publisher:	Springer
URL officiel: Official URL:	https://doi.org/10.1007/s00397-014-0801-3
Mention légale: Legal notice:	This is a post-peer-review, pre-copyedit version of an article published in Rheologica Acta (vol. 53, no. 10-11) . The final authenticated version is available online at: https://doi.org/10.1007/s00397-014-0801-3

Rheological and foaming behavior of polylactide with different molecular structures

N. Najafi[1,2], M. C. Heuzey[1], P. J.Carreau[1], D. Therriault[2], C. B. Park[3]

1- Research Center for High Performance Polymer and Composite Systems, CREPEC, , Chemical Engineering Department, Ecole Polytechnique, Montreal, Quebec, Canada
2- Research Center for High Performance Polymer and Composite Systems, CREPEC, ,Mechanical Engineering Department, Ecole Polytechnique, Montreal, Quebec, Canada
3- Microcellular Plastics Manufacturing Laboratory, Department of Mechanical and Industrial Engineering, University of Toronto, Toronto, Ontario, Canada

Abstract

In this work, a chain extender (CE), Joncryl © ADR, was added to a polylactide (PLA) at two concentrations, 0.4 and 0.7 wt%, using two different strategies. The rheological properties and foamability of the neat PLA and PLA containing the CE were studied. The steady and transient rheological properties of the neat PLA and CE-treated PLAs revealed that the introduction of the CE profoundly affected the melt viscosity and elasticity. The linear viscoelastic properties of CE-enriched PLAs suggested that a long chain branching (LCB) structure was formed from the reaction with the CE. LCB-PLAs exhibited an increased viscosity, more shear sensitivity, and longer relaxation time in comparison with the linear PLA. The LCB structure was also found to affect the transient shear stress growth and elongational flow behavior. LCB-PLAs exhibited a pronounced strain hardening, whereas no strain hardening was observed for the linear PLA. Batch foaming of the linear and LCB-PLAs was also examined at foaming temperatures of 130, 140, and 155 °C. The LCB structure significantly increased the integrity of the cells, cell density and void fraction

Keywords: polylactide, long chain branching, rheological properties, foaming behavior

1. Introduction

Biodegradable polymers have been extensively studied in the recent decades due to their remarkable properties (Drumright et al. 2000; Eslami and Kamal 2013; Garlotta 2001; Lunt 1998). Among them, polylactic acid or polylactide (PLA) is one of the most promising choices from both economic and environmental perspectives for commodity applications (Drumright et al. 2000; Garlotta 2001). Polylactide is a biodegradable, thermoplastic, aliphatic polyester synthesized from renewable resources such as corn, starch, and sugarcane using ring opening polymerization (Drumright et al. 2000; Garlotta 2001). PLA is expected to be one of the most competitive and favorable candidates as a substitute to petroleum-based polymers such as polystyrene (PS), polyethylene terephthalate (PET), and polyurethane (PU), which are either non-biodegradable (PS) or non-recyclable (Eslami and Kamal 2013; Garlotta 2001; Wang et al. 2012c; Wang et al. 2012d). PLA has been increasingly used in biomedical applications such as resorbable surgical sutures, implants, controlled drug delivery devices (Garlotta 2001; Soppimath et al. 2001; Theinsathid et al. 2009) and mass-production applications such as industrial and food packaging (Drumright et al. 2000; Garlotta 2001; Theinsathid et al. 2009). In addition to such versatile and valuable applications, the use of bio-based polymers is becoming more common in durable industries, particularly the automotive industry (So 2012). One of the key factors affecting the fuel consumption of automobiles is their weight, hence a reduction while maintaining the structural performance is one of the main challenges of the automotive industry (Airale et al. 2011). A potential approach to accomplish this objective is the use of the foaming technology. A microcellular foam is a polymeric foam with average cell size and cell density of 10 μm and 10^9 cells/cm^3, respectively (Pilla et al. 2009; Wang et al. 2012a). To achieve thermoplastic foaming, the polymer is first saturated with a gas under pressure and then

subjected to thermodynamic instability, leading to a rapid liberation of the gas and, consequently, cell nucleation. The nucleated cells start to grow until they stabilize (Mahmoodi et al. 2009; Zhu et al. 2006). The thermodynamic instability can be induced by either sudden pressure release or temperature increase (Mahmoodi et al. 2009; Zhu et al. 2006). The manufacturing of PLA foams has recently drawn great attention since this technique reduces the weight and cost of the final products (Lee and Ramesh 2004; Matuana and Diaz 2013; Pilla et al. 2009). However PLA was found to exhibit poor foamability (Matuana and Diaz 2013; Pilla et al. 2009; Wang et al. 2012d; You et al. 2013). The major obstacles in stabilizing the foamed cell structure of PLA are its low melt strength and melt elasticity, slow crystallization rate, and narrow processing window (Eslami and Kamal 2013; Matuana and Diaz 2013; Pilla et al. 2009; Wang et al. 2012a). Low viscosity and melt strength may lead to cell coalescence and coarsening and, hence, reduction of the cell density (Spitael and Macosko 2004). Crystallinity is another factor profoundly affecting cell nucleation and growth phenomena in PLA foaming (Wang et al. 2012b). The crystal phase may induce heterogeneous cell nucleation, resulting in an increased cell density and a reduced cell size (Lee and Ramesh 2004; Matuana and Diaz 2013; Wang et al. 2012a; Wang et al. 2012b). The melt strength of the resin is also increased by the presence of crystal domains, leading to suppression of cell coalescence, and more uniform cellular structure (Matuana and Diaz 2013; Wang et al. 2012a; Wang et al. 2012b). Different methods have been so far used to improve the melt strength and, subsequently, foamability of polymers; these include broadening of the molecular weight distribution (MWD) (Minegishi et al. 2001), controlled cross linking (Mitomo et al. 2005), blending (Eslami and Kamal 2013), introduction of a filler like nano-particles or wood flour (Matuana and Diaz 2013) and the formation of a long chain branching (LCB) structure (Pilla et al. 2009; Spitael and Macosko 2004; Wood-Adams et al. 2000). LCB is

believed to increase the melt strength and elasticity, leading to an increased ability to form and maintain a good cellular structure(Pilla et al. 2009; Spitael and Macosko 2004). Among the several research studies devoted to PLA foams (Di et al. 2005; Fujimoto et al. 2003; Mihai et al. 2010; Pilla et al. 2009; Pilla et al. 2010b; Seo et al. 2012; Taki et al. 2011; Wang et al. 2012a), the initial reports deal mainly with batch foaming (Di et al. 2005; Fujimoto et al. 2003; Taki et al. 2011), which is most useful to evaluate the impact of material composition and molecular structure on the cell morphology (Wang et al. 2012a). For example, Fujimoto *et al.* (Fujimoto et al. 2003) produced PLA and PLA-clay nanocomposite foams through a batch foaming process using CO_2 as a physical blowing agent (PBA). They investigated the impact of different types of clays on the foam structure and found that clay acted as a nucleating agent, decreasing foam density and cell size. Di *et al.* (Di et al. 2005) used butane diisocyanate (BDI) to achieve chain-extended PLAs. They studied the batch foaming of the modified PLAs using a mixture of CO_2/N_2 (20/80) as PBA. Their findings revealed that the cell density significantly increased (around 10 times), while its cell size was markedly reduced from 230 to 24 μm, depending on the molecular weight (M_W) of the chain-extended PLAs. The impact of the growing crystalline phase on cell nucleation in PLA-CO_2 batch foaming was considered by Taki *et al.* (Taki et al. 2011). To this end, they measured the ratio of cells nucleated around the spherulites to the total number of nucleated cells (n_c). It was found that n_c was strongly dependent on the type of spherulites formed and their surface area. On the other hand, continuous microcellular processing studies have also been carried out, including extrusion foaming (Mihai et al. 2010; Pilla et al. 2009; Wang et al. 2012a) and foam injection molding (Pilla et al. 2010b; Seo et al. 2012).The impact of LCB (Mihai et al. 2010) and different additives such as talc, nanoclay and nanosilica (Keshtkar et al. 2011; Nofar et al. 2012) on extrusion foaming of PLA was examined. The findings

demonstrated that an increased melt strength reduced the cell size while increasing the cell density. This improvement in continuous foaming processes cannot be only related to the molecular structure since the processing parameters such as applied shear, pressure drop and pressure drop rate would also be changed with the introduction of LCB. The incorporated fillers had an effective role on the PLA crystallization rate and on foamability, due to more cell nucleation sites. Nucleated crystals, conversely, acted as cell nucleation sites, leading to further increment of the cell density (Keshtkar et al. 2011; Nofar et al. 2012). The impact of hyper-branched polyesters (HBPs) and nanoclay on controlling the cellular morphology of microcellular PLA was investigated by Pilla *et al.* in foam injection molding (Pilla et al. 2010b). Depending on the concentration of HBPs and nanoclay added to PLA, they found that the cell density increased up to 10 times, while the cell size and weight of microcellular samples was reduced by 4 times and 16 %, respectively.

This paper aims at illustrating how LCB and molecular structure impact the melt rheology and batch foaming behavior of PLA. To this end, LCB-PLAs were prepared in the presence of a multifunctional chain extender using two different processing strategies. Then, their rheological properties and foamability were investigated in details and correlated to their molecular architecture.

2. Experimental

2-1. Material

The polylactide (PLA) used in this study, PLA 3001D, was purchased from NatureWorks LLC Co. (USA). The selected grade is a semi-crystalline linear polymer with an *L*-lactide to *D*-lactide ratio of 98.5: 1.5 (Kramschuster and Turng 2009) and its melt flow rate (MFR) is 22 g/10 min under a load of 2.16 kg at 210 °C (ASTM D1238), as reported by the manufacturer. Joncryl®

ADR-4368F, supplied by BASF (Germany), is a modified acrylic copolymer with epoxy functions that was used as a chain extender in this work.

2-2. Material Processing

Melt compounding of PLA with chain extender (CE) was performed using a counter-rotating Brabender Plasti-Corder® internal mixer. Before compounding, the PLA was dried at 70 °C in a vacuum oven for 24 h. The dried PLA was then directly mixed in the molten state with 0.4 and 0.7 wt% CE in the internal mixer at a set temperature of 185 °C, a procedure called strategy S1. The mixing was conducted under a nitrogen atmosphere at a rotation speed of 100 rpm for 10 min, after which a relatively steady state torque was established. The neat PLA, as received, was dried and used as a reference in this study. To further examine the impact of CE and molecular topology, a PLA containing 0.4 wt% of CE was prepared using a second approach, strategy S2, in which the PLA was first compounded with 0.8 wt% CE in the internal mixer for 10 min at conditions stated above. The resulting blend was dried in a vacuum oven (70 °C) for 24 h. Then, in the second run, it was mixed with the neat PLA at a weight ratio of 50:50 using the same operating conditions. The processed materials were placed in a vacuum oven (70 ºC) for 24h. To determine the uniaxial elongational and shear rheological properties, rectangular sheets of $18\times10\times1$ mm³ and disk-shaped samples of 25 mm diameter and 1.5 mm thickness, respectively, were prepared by compression molding under a nitrogen atmosphere at 185 ºC and 20 MPa for 8 min, followed by fast cooling to ambient temperature. The prepared samples were stored in a desiccator until use.

For batch foaming, disk-shaped samples of 20 mm diameter and 0.6 mm were prepared and placed in a high pressure vessel hosted in a MCR501 rheometer (Anton Paar, Austria). The samples were first heated up to 180 ºC and held at that temperature for 10 min. The molten

polymers were then pressurized with CO_2 at a pressure of 9 MPa at the same temperature for 30 min. While keeping the pressure constant, the processing temperature was reduced to the foaming temperature (T_f), ranging from 130 to155 ^{o}C and held for 90 min. Thereafter, the CO_2 pressure was rapidly reduced to supersaturate the specimen with gas, leading to the formation of foamed cells.

2-3. Characterization

Rheological measurements

The prepared disk-shaped samples were used to measure steady and dynamic shear rheological properties. Both steady-state viscosity (η) and small amplitude oscillatory shear (SAOS) data were measured at 180 °C under a nitrogen atmosphere using a MCR-301 rotational rheometer (Anton Paar, Austria) with a parallel flow plate geometry of 25 mm diameter. A 0.95 mm gap was used to measure the steady-state viscosity at various shear rates ($\dot{\gamma}$) ranging from 0.01 to 1 s^{-1}. A 1.1 mm gap was used for the SAOS measurements and the strain amplitude was set at 0.05, large enough to give a reliable signal while keeping the measurement in the linear viscoelastic regime. Time sweep tests were first performed at a frequency of 6.28 rad/s, indicating that maximum variation in dynamic data was less than 8 % over the time frame of the experiments (25 min). The rheological material functions such as complex viscosity (η*), elastic (G') and loss modulus (G'') were measured in the frequency range of 0.628 to 628 rad/s.

Nonlinear transient rheological measurements were also carried out using a strain controlled Rheometric Scientific ARES rheometer (TA Instruments, USA). Stress growth experiments were conducted in a parallel plate geometry with a diameter of 25 mm and a gap of 1.1 mm under a nitrogen atmosphere at 180 ^{o}C and a range of shear rates (($\dot{\gamma}$) = 0.1, 1, and 2 s^{-1}). For each test, a fresh sample was used and preheated 10 min at the set temperature. Finally, the prepared

rectangular sheet samples were used to measure the uniaxial elongational viscosity. This measurement was carried out using the ARES rheometer equipped with a SER universal testing platform (Xpansion Instruments, USA). Measurements were performed under a nitrogen atmosphere over a range of Hencky strain rates from 0.3 to 20 s^{-1} while the temperature was respectively kept at 170 and 180 °C for the neat PLA and CE-enriched PLAs. A lower temperature of 170 °C was selected for the neat PLA because its melt viscosity at 180 °C was too low and insufficient for extensional testing. A sufficient time (5 min) was elapsed prior to starting the test to ensure thermal equilibrium within the specimen.

Morphological characterization

The density of the foamed samples was measured using the water displacement method at ambient pressure and temperature based on the standard ASTM792-00. The void fraction was determined using Eq. 1 (Lee and Park 2006).

$$V_f = \left(1 - \frac{\rho_f}{\rho_s}\right) \times 100 \tag{1}$$

where ρ_f and ρ_s are the density of the foamed and solid sample (1.25 g/cm^3), respectively. Cell morphology of the foamed samples was observed using a JSM-840 scanning electron microscope (SEM) (JEOL, USA) operated at accelerating voltage of 10 kV. Prior to the SEM observations, the samples were freeze-fractured in liquid nitrogen and sputter-coated with a thin layer of gold. A quantitative analysis of the average cell size and cell density of 200 cells was carried out using an image analysis tool (ImageJ, NIH). The cell density, or the number of cells per unit volume (cm^3) of the original unfoamed polymer, was calculated using Eq. 2 (Naguib et al. 2002).

$$\text{Cell density} = \left(\frac{n}{A}\right)^{3/2} \times \left(\frac{\rho_p}{\rho_f}\right) \tag{2}$$

where n, and A are the number of the cells in the micrograph and area of the micrograph (cm^2), respectively.

3. Results and Discussion

3-1. Rheological properties

Viscoelasticity is typically found to significantly influence the foamability of thermoplastic polymers (Gendron 2005; Lee and Ramesh 2004). The viscoelastic properties of molten polymers are markedly affected by molecular weight (M_w), molecular weight distribution (MWD), and the entanglement density (Gendron 2005; Lee and Ramesh 2004). Low M_W and narrow MWD resins exhibit inadequate rheological properties and narrow processing window for foaming (Lee and Ramesh 2004). The steady-shear viscosity (η), complex viscosity (η^*) and elastic modulus of the neat PLA and PLA prepared with various concentrations of CE using the two different compounding strategies are plotted as functions of shear rate ($\dot{\gamma}$) and frequency (ω) in Fig. 1. The solid lines in Fig.1a represent the fits of the Carreau-Yasuda model (Carreau et al. 1997) used to extrapolate the zero-shear viscosity (η_0), reported in Table 1. We note the Cox-Merz rule is valid for all the samples. The Carreau-Yasuda model describes well all sets of data. Both η and η^*, as shown in Fig. 1a, gradually decrease with increasing $\dot{\gamma}$ and/or ω, exhibiting the typical shear-thinning behavior of polymer melts. The neat PLA is characterized by a low complex viscosity, shear viscosity, shear sensitivity and a broad Newtonian plateau.

The incorporation of CE into the neat PLA, however, changes considerably its rheological response. The magnitude of the complex and steady shear viscosity is increased by two orders of magnitude at low frequencies or shear rates, depending on the CE content. Meanwhile, the transition from a Newtonian plateau to the so-called shear-thinning regime shifts to a lower frequency or shear rate, as the CE content is increased, suggesting the presence of a

microstructure with a long relaxation time. The observed change in the viscosity behavior can be attributed to the macromolecular chain extension and branching, as discussed in a previous publication (Najafi et al. 2012) and summarized below. In comparison with the PLA treated by 0.4 wt% CE and prepared by strategy S1, the sample prepared by strategy S2 exhibits a higher viscosity and elasticity at very low shear rates and frequencies. The reason of this increase is also explained below.
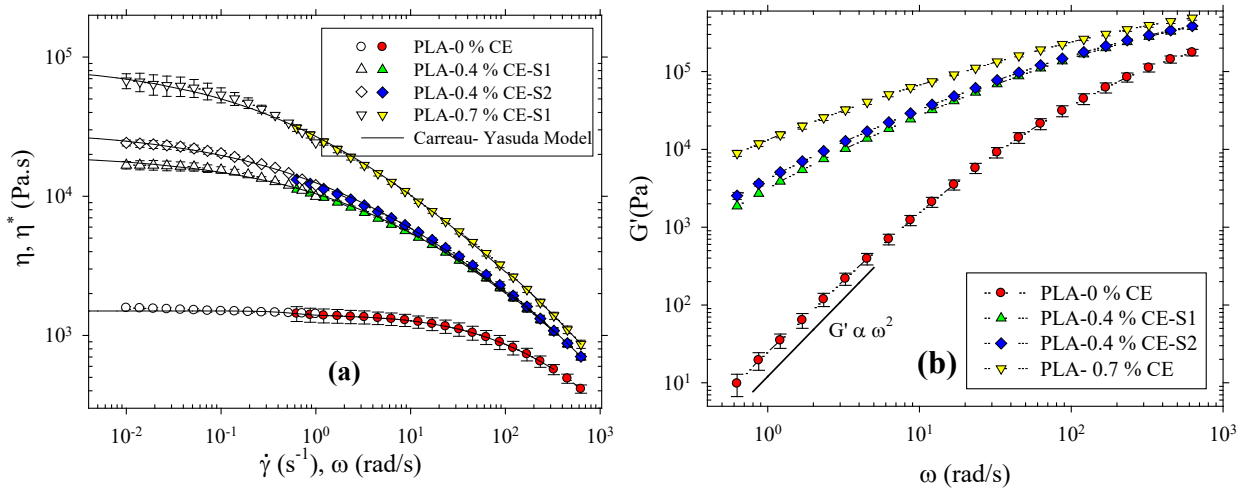

Fig. 1 The linear viscoelastic properties (a) shear (open symbols) and complex viscosity (filled symbols) (b) storage modulus of the neat and CE-enriched PLAs at 180 °C.

Structural changes in polymeric materials can be evaluated with the linear viscoelastic properties, considering that they are very sensitive to topological structure of macromolecular chains. The storage modulus (G') is even more sensitive to structural changes in viscoelastic materials (Coppola et al. 2006). G' data of the neat PLA and CE-enriched PLAs are presented in Fig. 1b as a function of ω. G' of PLAs treated by CE is larger than that of the neat PLA in the entire range of ω and increases with increasing CE content. The storage modulus of polymeric materials with a linear macromolecular structure theoretically grows with square of ω in the terminal zone (i.e. at low frequencies where $G' \sim \omega^2$), where only the longest relaxation time contributes to the viscoelastic behavior (Tian et al. 2006). The slope of G' versus ω of the neat

PLA and CE-enriched PLAs were calculated in the terminal zone. The value for the neat PLA is 1.88, quite close to the theoretical value of 2, confirming the linear structure of the polymer. However, the slope for S1 and S2 compounded samples and the PLA containing 0.7 wt% of CE is reduced to 1.06, 1, and 0.80, respectively. The observed non-terminal behavior can be ascribed to a long chain branching structure. This evidence was used in (Eslami and Kamal 2013; Tian et al. 2006; Wood-Adams et al. 2000) to verify the formation of long chain branching structure.

To gain further understanding of the polymer molecular structure after the CE incorporation, the reduced complex viscosity and loss angle were considered as a function of shifted frequency using the zero-shear viscosity, as illustrated in Fig. 2. A narrower Newtonian plateau and a broad transition region between the Newtonian plateau and the power-law zone, as observed in Fig. 2a for the CE-PLA samples, can be caused by the broadening of the MWD as discussed in (Najafi et al. 2012; Wood-Adams et al. 2000).
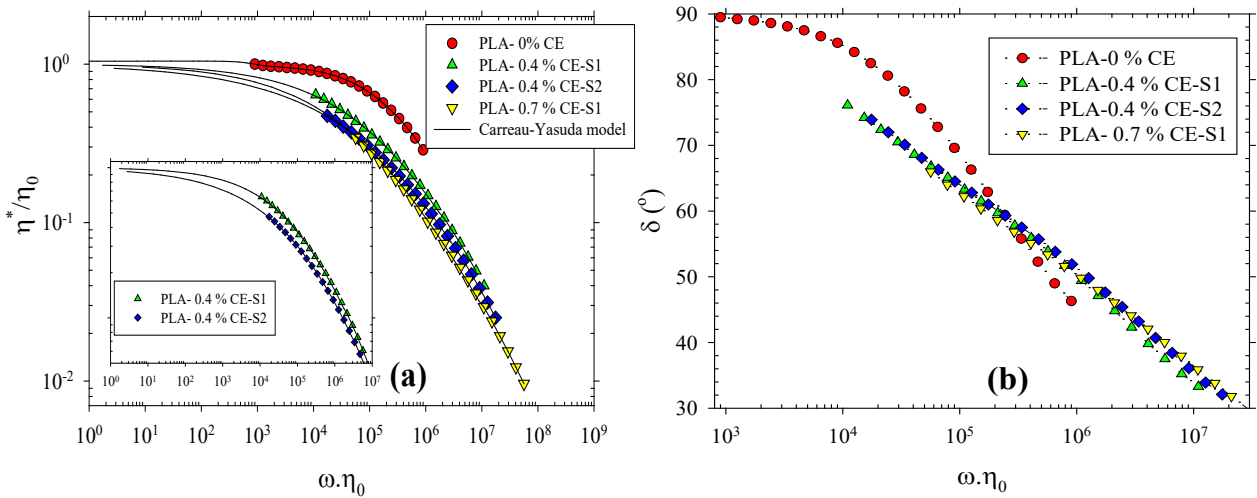

Fig. 2 The shifted rheological properties (a) complex viscosity and (b) loss angle of neat and CE-enriched PLAs at 180 °C as a function of shifted frequency.

Due to the presence of relaxation modes at long times related to branched chains in a LCB structure, the shape of the loss angle curve also prominently changes (Najafi et al. 2012; Wood-

Adams et al. 2000). The results in Fig. 2b reveal that the molecular structure of CE-enriched systems significantly differ from that of the neat PLA and is consistent with the presence of a long chain branching (LCB) structure, as extensively discussed in our previous work (Najafi et al. 2012). The formation of the LCB structure is responsible for the increased M_W and MWD, leading to increased melt strength, elasticity, shear sensitivity, and consequently, as we will see later, to improved foamability.

The CE-enriched PLA prepared by strategy S2 shows a slightly broader transition region (see inset of Fig. 2a), and consequently, a broader MWD as compared with that prepared by strategy S1. In the S2 compounded sample, increased CE content (in the first run) favored the formation of a highly LCB structure in comparison with that prepared using S1. The longer residence time due to the second compounding step may also influence the extent of reaction of the chain extender.
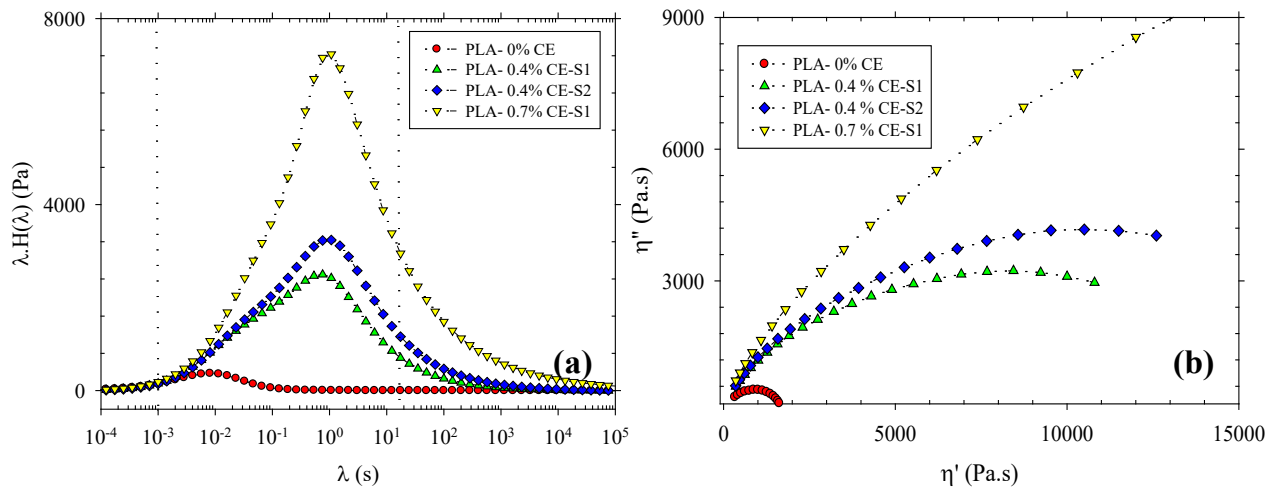

Fig. 3 (a) Weighted relaxation spectra and (b) Cole-Cole plots of the neat and LCB-PLAs prepared using the two different strategies.

To examine the impact of LCB on the compound's relaxation behavior, the time-weighted relaxation spectra, $\lambda H(\lambda)$ of the linear and LCB-PLAs were calculated using the SAOS data via

the non-linear regularization (NLREG) method and are illustrated in Fig. 3a. The dashed, vertical lines show the experimental window. The area under the relaxation time spectra represents the zero-shear viscosity (η_0) of the melt and the values are given in Table 1.

There is a good agreement between these values and those obtained using the Carreau-Yasuda model, implying that the calculated time-weighted relaxation spectra are accurate. As the results show, the formation of the LCB-structure dramatically changes the shape and peak location of the relaxation spectrum. This shift mainly results from the change of relaxation mechanisms (He et al. 2004). While reptation is the main relaxation mechanism for linear chains (Van Ruymbeke et al. 2005), branched chains relaxes by arm retraction, leading to a retardation of chain movement along their backbone (He et al. 2004) and, consequently, broadening of the relaxation spectrum.

Table 1 The zero-shear viscosity of the neat and CE-enriched PLAs at 180 °C calculated using (a) the Carreau-Yasuda model and (b) the area under the relaxation time distribution

Composition	η_0 (kPa.s)[a]	η_0 (kPa.s)[b]
PLA-0 wt% CE	1.4 ±0.1	1.3
PLA-0.4 wt% CE-S1	20.1 ±1.0	19.4
PLA-0.4 wt% CE-S2	30.1 ±1.4	30.5
PLA-0.7 wt% CE	89.8 ±2.8	84.3

In comparison with the 0.4 wt% CE-PLA prepared using strategy S1, the S2 sample exhibits a slightly broader relaxation spectrum as shown in Fig. 3a due to a more developed LCB structure. Increasing the CE content from 0.4 to 0.7 wt% further increases the fraction of branched macromolecules, leading to the broadening of the relaxation spectrum.

To further analyze the relaxation process, Cole-Cole plots (η'' versus η') (He et al. 2004; Tian et al. 2006) are presented in Fig. 3b. The Cole-Cole plot of the linear PLA is found to be semicircular. Depending on the degree of LCB, the plots for the CE-enriched PLAs deviate from the semicircular shape and exhibit more evident upturning at high viscosity values, implying the

existence of LCB macromolecules. This behavior was also observed by others (He et al. 2004; Tian et al. 2006) for polymers with long chain branching.

The transient flow properties were also studied since they play an important role in the foaming phenomenon. The normalized shear stress growth coefficient ($\eta^+(t)/\eta$) of the linear and LCB-PLAs at different shear rates are illustrated in Fig. 4. The viscosity at steady state was reported in Fig. 1a.
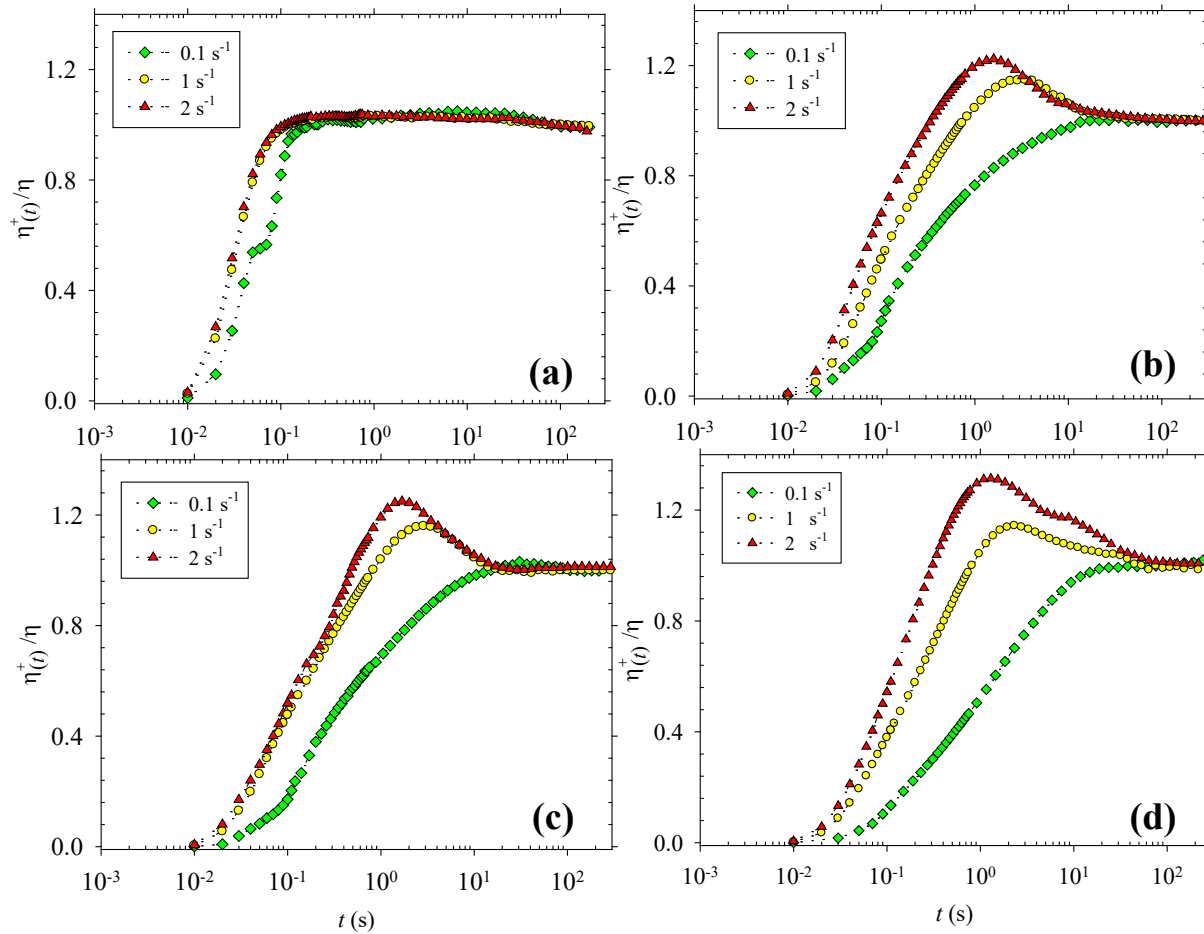

Fig. 4 Normalized stress growth coefficient of (a) the neat PLA, (b) PLA containing 0.4 wt% CE prepared using strategy S1, (c) PLA containing 0.4 wt% CE prepared using strategy S2, and (d) PLA containing 0.7 wt% CE prepared by strategy S1 at 180 °C and three different shear rates.

The origin of the transient response is considered to be the orientation of the macromolecules and decreases in the entanglement density (Robertson et al. 2002). No significant overshoots are observed for the neat PLA, even at the larger shear rate as shown in Fig. 4a, suggesting the low entanglement density of the polymer. Contrary to the neat PLA, the CE-enriched PLAs (Fig. 4b-d), however, exhibit prominent overshoots in their transient shear response. For instance, an overshoot of roughly 25 and 35 % above the steady state value is observed at a shear rate of 2 s^{-1} for PLA containing 0.4 and 0.7 wt % CE, respectively. This is caused by the increased entanglement density as a consequence of long chain branching. The stress growth behavior of the PLA containing 0.4 wt% CE prepared using the two strategies is about the same at these shear rates. The stress overshoot becomes more pronounced and occurs at shorter time with increasing shear rate. The required shearing time to reach the steady state also increases from 0.3 s for the neat PLA to 30 and 70 s for the PLA containing 0.4 and 0.7 wt% CE, respectively. The enhanced entanglement density in LCB-macromolecules (Wever et al. 2013) inhibits the motion of the polymer chains and delays their relaxation. Fig. 5 presents the transient uniaxial elongational viscosity of the neat PLA, measured at 170 °C, and the LCB-PLAs, measured at 180 °C , at different strain rates. Even though cell expansion in foaming is controlled by biaxial elongational viscosity, the uniaxial behavior can provide useful information about melt strength. The dashed lines illustrate the transient shear viscosity predicted from the linear viscoelasticity data using the generalized Maxwell model and multiplied by three. Note that at very early stages of the test, i.e. at times less than 0.05 s, the measured extensional viscosity of all samples is less than that predicted by the time-dependent shear viscosity. This is most likely due to instrument limitations in reaching instantaneously the set strain rate. The elongational viscosity of the neat PLA increases until it reaches a steady value. As expected for a molten linear polymer, strain

hardening (SH) is not observed for the neat PLA (Fig. 5a) confirming the results of the literature (Eslami and Kamal 2013; Matuana and Diaz 2013; Wang et al. 2012c). In contrast, the elongational viscosity of the LCB-PLAs profoundly deviates from the linear viscoelasticity (Fig. 5b and c) at all strain rates and shows an upturn behavior (SH) at longer times. This upturn behavior occurs faster as the strain rate is increased. In fact, increased entanglements associated with LCB hinder the chain contraction during extension, leading to a pronounced SH behavior (Lee and Ramesh 2004).
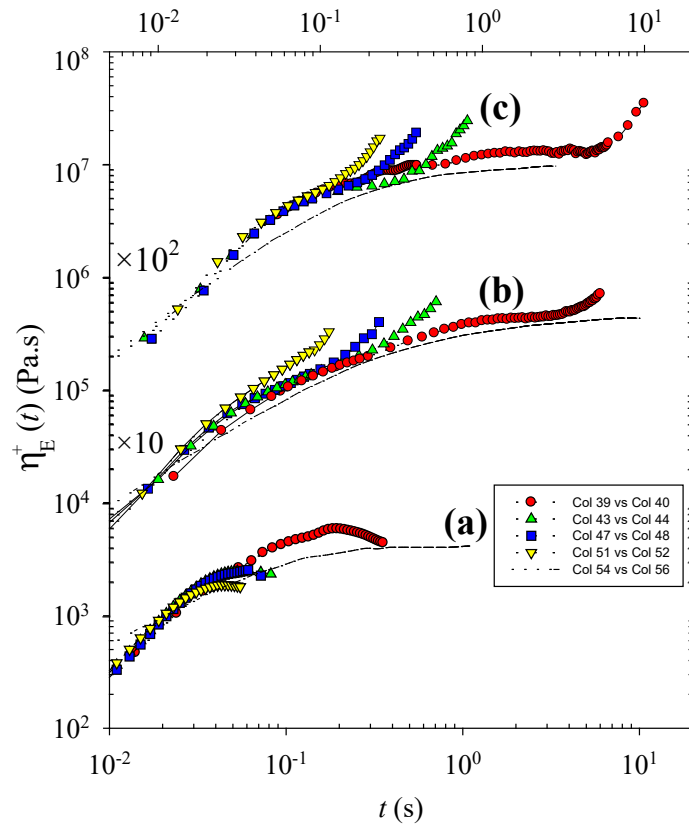

Fig. 5 Transient elongational viscosities of (a) neat PLA at 170 °C and (b) LCB-PLA containing 0.4 wt% of CE prepared using strategy S2 , and (c) LCB-PLA containing 0.7 wt% of CE at 180 °C and different strain rates. The transient elongational viscosity of LCB-PLAs containing 0.4 wt% CE prepared using strategy S1 showed a similar trend with those prepared using S2 and, hence, is not presented.

3-3. Foaming behavior

The foaming behavior of the linear and LCB-PLAs is investigated at temperatures of 130, 140, and 155 °C. Representative SEM images of the fractured surfaces of foamed samples are shown in Fig. 6. Contrary to the linear PLA, LCB-PLAs are not foamed effectively at the foaming temperature of 130 °C (see the first column of Fig. 6) due to too high stiffness and strength of the polymer molten phase. Moreover, isothermal and non-isothermal crystallization studies revealed that the crystallization rate and degree of LCB-PLAs were much larger than those of the linear counterpart (data are not presented here for brevity). Considering that the foaming temperature is below the melting point and close to the crystallization temperature, LCB polymer melts, hence, solidify too quickly before the nucleated cells could grow. However at higher foaming temperatures of 140 and 155 °C, the contribution of crystallization to the cellular structure cannot be assessed since they are above the melting point (the melting point of PLA is depressed from 160 to 135 °C at this pressure (9 MPa) (Nofar et al. 2013)). As shown in Fig. 6b-d the LCB-PLAs exhibit more uniform cells with smaller size and larger cell density at 140 and 155 °C in comparison with the linear PLA.

As a result of long chain branching, the melt strength of PLA is improved and the cellular structure of the foams becomes well-developed and uniform. The volume expansion ratios of the linear and LCB-PLA foams, defined as the ratio of polymer density (1.25 g/cm^3) to foam density, was measured at different foaming temperatures and used to characterize the void fraction (Eq. 1). Fig. 7a depicts the void fraction of the resulting foams with respect to the foaming temperature. The obtained results indicate that the expansion ratio and, consequently, the void fraction is strongly dependent on the LCB content and processing conditions. The void fraction of the foamed neat PLA decreases from 0.75 to 0.17 with increasing foaming temperature from 130 to 155 °C. In contrast with the neat PLA, the void fraction of LCB-PLAs is enhanced with

increasing foaming temperature. The void fraction of S1 (0.12 at 130 ℃) and S2 (0.08 at 130 ℃) compounded samples and the PLA containing 0.7 wt% CE (0.08 at 130 ℃) increases to 0.90, 0.88, and 0.85, respectively, as the foaming temperature is raised to 155 ℃.
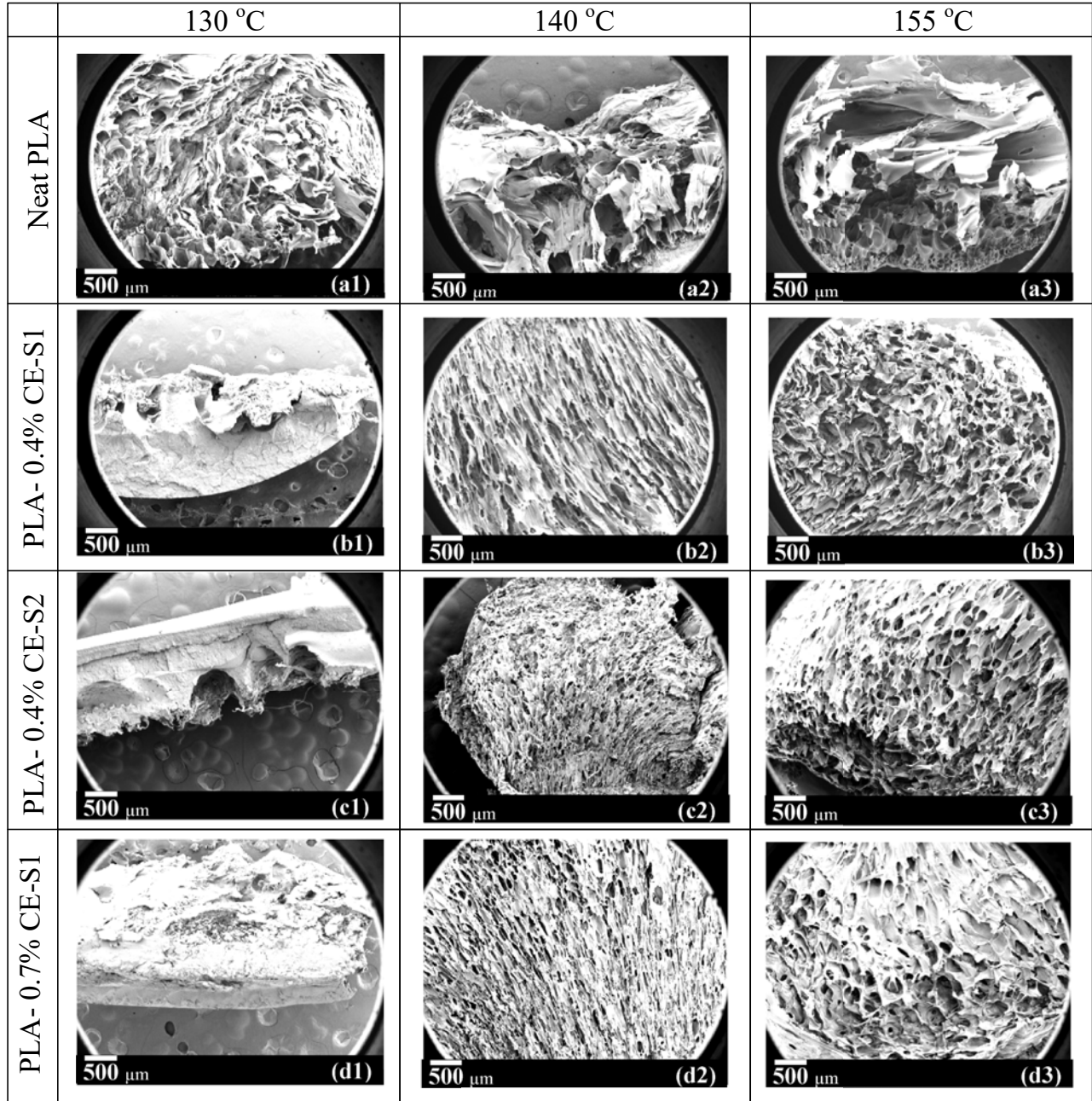

Fig. 6 Representative SEM micrographs of cryo-fractured surfaces of (a) neat PLA (b) PLA containing 0.4 wt% CE prepared using strategy S1 (c) PLA containing 0.4 wt% CE prepared using strategy S2, and (d) PLA containing 0.7 wt% CE prepared by strategy S1 at different foaming temperature.

Naguib *et al.* (Naguib et al. 2004) investigated the fundamental mechanisms governing the expansion behavior of polymeric foams. They found that the final expansion ratio was governed either by the gas loss that occurred through diffusion out of the foam or by the crystallization and melt stiffening of the polymeric matrix (Lee et al. 2005; Naguib et al. 2004). If the foaming temperature was too high, the solidification time became too long. Therefore, the gas that diffused out of the melt towards the nucleated cells had enough time to escape out of the foam. Under these conditions, the maximum expansion ratio was governed by gas loss and it decreased with increasing processing temperature. However, if the processing temperature was too low, the maximum expansion ratio was controlled by solidification and increased with temperature (Naguib et al. 2004). According to these investigations, the expansion ratio and void fraction of the samples, excluding the neat PLA, are governed by melt stiffening and crystallization, at least at 130 °C. As the foaming temperature increases, the degree of crystallization, melt viscosity and, thus, melt strength of the polymer decrease, allowing the created cells to be further expanded. A reverse trend in the case of the neat PLA is illustrated in Fig 7a. The SEM images presented in Fig. 6a clearly reveal that increasing the foaming temperature from 130 to 155 °C promotes cell rupture due to a reduced melt viscosity and elasticity. As a result, most of the gas escapes from the foam during the expansion process. The amount of gas retained in the foam, thus, decreases, leading to a reduction of the gas pressure for expansion and a decreased void fraction. Although the effect of LCB on void fraction is striking when compared to linear PLA, the differences between the various LCB-PLAs are within the experimental uncertainty at all foaming temperatures.

The cell density (Eq. 2) and cell size are reported in Fig. 7b and c, respectively. The cell density of the neat PLA continuously decreases from 7×10^5 to 4×10^4 cells/cm^3 (more than one order of

magnitude) as the foaming temperature is raised from 130 to 155 °C. The increase of the foaming temperature decreases the melt strength of the polymer, leading to severe cell coalescence and cell rupture (Lee et al. 2005; Nofar and Park 2014). Consequently, most of the nucleated cells are broken during expansion, as shown in Fig. 6a and the cell density of the foam is reduced by more than 17 times. Another possibility is the crystal-induced cell nucleation at a lower temperature due to the stress variations around the stiffened crystal nuclei (Garancher and Fernyhough 2012; Wong et al. 2013). The cell density of LCB PLAs is less than 4×10^3 cells/cm^3 at a foaming temperature of 130 °C. As mentioned earlier, too high stiffness and strength of the branched polymer melts at 130 °C make it difficult for the cells to nucleate and grow. However, with increasing foaming temperature to 140 °C (see in Fig. 6b-d), the cell density increases to 9.5×10^6, 2.1×10^7, and 1.2×10^7 cells/cm^3 in PLA containing 0.4 wt% CE with strategy S1, with strategy S2, and the PLA containing 0.7 wt% CE, respectively. The incorporation of the chain extender into the neat PLA enhances the cell density by two orders of magnitude.
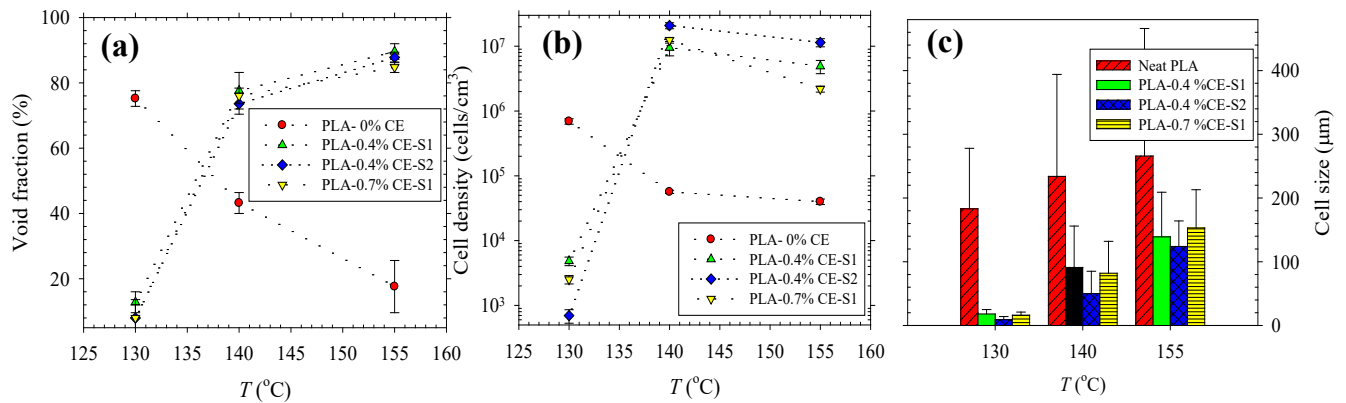

Fig. 7 The effect of long chain branching and foaming temperature on (a) void fraction, (b) cell density, and (c) cell size of PLA foams.

The increased cell density of LCB-PLAs is attributed to higher melt strength and strain hardening behavior, resulting from long chain branching, that stabilize the nucleated cells by

minimizing cell coalescence. A comparison of the cell density for PLA containing 0.4 wt% CE indicates that the S2 sample has a higher cell density (two times) than the S1 sample. The results presented in Fig. 1a reveal that the melt viscosity of the LCB-PLA containing 0.4 wt% CE prepared using strategy S2 was higher than sample S1, particularly at low frequencies or shear rate. The increase in cell density can be explained by a decreased gas diffusion rate with increasing polymer melt viscosity (Wong et al. 2007). This is in agreement with results published by Di *et al.* (Di et al. 2005) in PLA treated with butane diisocyanate (BDI). As extensively discussed by Park *et al.* (Park et al. 1995), there is a competition between cell nucleation and cell growth. They reported that the real pressure drop and cell nucleation time were not instantaneous and happened over a finite time period. During the course of the pressure drop, some stable cells nucleated early and, then, the gas in solution in the polymer melt diffused to the nucleated cells. As the pressure further dropped, the system would either just expand the existing cells by gas diffusion or nucleate additional cells while expanding the existing cells. An increase of the melt viscosity makes difficult the gas diffusion and mass transfer into the nucleated cells. Thus, the gas in solution preferentially nucleates new microcells rather than diffusing to the existing cells, leading to an increase of the cell density. In comparison with the S2 compounded sample, PLA containing 0.7 wt% CE shows a lower cell density, even though it has a higher melt strength. The increase of the free volume resulting from branching (Gong et al. 2005) is most likely responsible for the observed decline in the cell density. A higher degree of branching, obtained after incorporation of 0.7 wt% CE further increases the free volume between the chains and, thus, increases the gas diffusion rate. As a result, more gas in solution in the melt migrates preferentially to the existing cells rather than nucleating new bubbles, causing a decreased cell density. Comparing the results in Fig. 7b also show that the cell density of LCB-PLAs tends to

decrease by more than 50 % as the foaming temperature is increased from 140 to 155 °C. The reduction of the cell density with respect to temperature can be related to many factors such as a reduction in gas solubility (Mahmood et al. 2014), a decrease of the melt strength, an increase of the gas diffusion rate (Pilla et al. 2010a; Wong et al. 2007), and a decreased number of the crystal nuclei that can affect cell nucleation (Wong et al. 2013).

The average cell size of the foamed samples is determined by measuring the maximum diameter of 200 cells in SEM micrographs and reported in Fig. 7c. The average cell size for the linear and LCB-PLAs increases with foaming temperature due to enhanced gas diffusivity and reduction of the melt strength. This, in turn, promotes the gas diffusion into the nucleated cells and decreases the resistance for cell growth (Wong et al. 2007). At the same foaming temperature, LCB-PLAs exhibit a smaller cell size than the linear PLA. For instance, at a foaming temperature of 140 °C the average cell size is reduced from 234 μm in neat PLA to 91, 50, and 82 μm in the PLA containing 0.4 wt% CE prepared using strategies S1 and S2, and the PLA containing 0.7 wt% CE, respectively. This reduction might be due to increased melt strength of the LCB-PLAs as a result of branching. The cell wall stability is improved with increasing melt strength, thereby decreasing the cell coalescence and average cell size (Nofar and Park 2014). Among the investigated compositions, the PLA containing 0.4 wt% CE prepared using strategy S2 exhibits the smaller average cell size at all foaming temperatures. Considering that more cells are nucleated in this case (higher cell density), there is less gas available for each cell to grow (Pilla et al. 2010a), leading to the formation of cells with smaller size.

Conclusion

In this study, long chain branched (LCB) PLAs were prepared by a melt grafting reaction in the presence of a multi-functional chain extender (CE). Two different concentrations, 0.4 and 0.7

wt%, CE were added to the neat PLA to achieve different degrees of branching. LCB-PLA containing 0.4 wt% CE were prepared using two strategies called S1 and S2. The rheological and foaming behavior of linear and resulting LCB-PLAs was investigated. The steady and transient rheological properties of the linear and LCB-PLAs revealed that the introduction of the CE profoundly affected the melt viscosity and elasticity. The LCB-PLAs exhibited an increased viscosity, shear sensitivity, and longer relaxation time in comparison with linear PLA. A prominent overshoot was found in the transient shear response of CE-enriched PLAs due to an increase of the entanglement density and, consequently, melt elasticity. The incorporation of CE into PLA and the resulting LCB, moreover, led to a strong strain hardening behavior in uniaxial elongational flow whereas no strain hardening was observed for the linear PLA.

The batch foaming of the linear and LCB-PLAs was conducted using CO_2 at different foaming temperatures ranging from 130 to 155 °C. The impact of molecular structure and foaming temperature on the cell morphology, void fraction, cell density, and cell size were examined. It was found that increased melt strength and elasticity, resulting from branching, strongly promoted the cell uniformity, cell density and void fraction. In general, the cell growth was accelerated with increasing foaming temperature. The cell density of LCB-PLAs was enhanced as the foaming temperature increased up to 140 °C, beyond which the cell density decreased. Among the investigated compositions, PLA containing 0.4 wt% CE prepared by strategy S2 provided smaller cell size and higher cell density than the others. As a result, the foaming temperature of 140 °C and chain extender content of 0.4 wt%, added based on the strategy S2, were found the optimum conditions to achieve finer and denser cell morphology in PLA foams.

References

Airale A, Carello M, Scattina A (2011) Carbon fiber monocoque for a hydrogen prototype for low consumption challenge Material Wiss Werkst 42:386-392 doi:10.1002/mawe.201100793

Carreau PJ, De Kee DCR, Chhabra RP (1997) Rheology of Polymeric Systems Principles and Applications Hanser-Garner Publications,

Coppola S, Acierno S, Grizzuti N, Vlassopoulos D (2006) Viscoelastic Behavior of Semicrystalline Thermoplastic Polymers during the Early Stages of Crystallization Macromolecules 39:1507-1514 doi:10.1021/ma0518510

Di Y, Iannace S, Di Maio E, Nicolais L (2005) Reactively Modified Poly(lactic acid): Properties and Foam Processing Macromol Mater Eng 290:1083-1090 doi:10.1002/mame.200500115

Drumright RE, Gruber PR, Henton DE (2000) Polylactic Acid Technology Adv Mater 12:1841-1846 doi:10.1002/1521-4095(200012)12:23<1841::aid-adma1841>3.0.co;2-e

Eslami H, Kamal MR (2013) Effect of a chain extender on the rheological and mechanical properties of biodegradable poly(lactic acid)/poly[(butylene succinate)-co-adipate] blends J Appl Polym Sci 129:2418-2428 doi:10.1002/app.38449

Fujimoto Y, Ray SS, Okamoto M, Ogami A, Yamada K, Ueda K (2003) Well-Controlled Biodegradable Nanocomposite Foams: From Microcellular to Nanocellular Macromol Rapid Comm 24:457-461 doi:10.1002/marc.200390068

Garancher J-P, Fernyhough A (2012) Crystallinity effects in polylactic acid-based foams J Cell Plast 48:387-397 doi:10.1177/0021955x12448804

Garlotta D (2001) A literature review of poly(lactic acid) J Polym Environ 9:63-84 doi:Unsp 1566-2543/01/0400-0063/0

Gendron R (ed) (2005) Thermoplastic foam processing, principles and development. CRC Press,

Gong W, Mai Y, Zhou Y, Qi N, Wang B, Yan D (2005) Effect of the Degree of Branching on Atomic-Scale Free Volume in Hyperbranched Poly[3-ethyl-3-(hydroxymethyl)oxetane]. A Positron Study Macromolecules 38:9644-9649 doi:10.1021/ma051026j

He C, Wood-Adams P, Dealy JM (2004) Broad frequency range characterization of molten polymers J Rheol 48:711-724 doi:doi:http://dx.doi.org/10.1122/1.1763943

Keshtkar M, Nofar M, Majithiya K, Park CB, Carreau P Foaming behavior of PLA/nanocolay nanocomposites in continious extrusion. In: BioFoams, Itally, 2011.

Kramschuster A, Turng L-S (2009) An injection molding process for manufacturing highly porous and interconnected biodegradable polymer matrices for use as tissue engineering scaffolds J Biomed Mater Res Part B: Appl Biomate 92B:366-376 doi:10.1002/jbm.b.31523

Lee JWS, Park CB (2006) Use of Nitrogen as a Blowing Agent for the Production of Fine-Celled High-Density Polyethylene Foams Macromol Mater Eng 291:1233-1244 doi:10.1002/mame.200600203

Lee JWS, Wang K, Park CB (2005) Challenge to Extrusion of Low-Density Microcellular Polycarbonate Foams Using Supercritical Carbon Dioxide Ind Eng Chem Res 44:92-99 doi:10.1021/ie0400402

Lee ST, Ramesh NS (eds) (2004) Polymeric Foams; Mechanisms and Materials. CRC Press LLC,

Lunt J (1998) Large-scale production, properties and commercial applications of polylactic acid polymers Polym Degrad Stabil 59:145-152 doi:http://dx.doi.org/10.1016/S0141-3910(97)00148-1

Mahmood SH, Keshtkar M, Park CB (2014) Determination of carbon dioxide solubility in polylactide acid with accurate PVT properties J Chem Thermodyn 70:13-23 doi:http://dx.doi.org/10.1016/j.jct.2013.10.019

Mahmoodi M, Behravesh AH, Rezavand SAM, Golzar M (2009) Theoretical and visual study of bubble dynamics in foam injection molding Polym Eng Sci 50:561-569 doi:10.1002/pen.21565

Matuana LM, Diaz CA (2013) Strategy To Produce Microcellular Foamed Poly(lactic acid)/Wood-Flour Composites in a Continuous Extrusion Process Ind Eng Chem Res 52:12032-12040 doi:10.1021/ie4019462

Mihai M, Huneault MA, Favis BD (2010) Rheology and extrusion foaming of chain-branched poly(lactic acid) Polym Eng Sci 50:629-642 doi:10.1002/pen.21561

Minegishi A, Nishioka A, Takahashi T, Masubuchi Y, Takimoto J-i, Koyama K (2001) Uniaxial elongational viscosity of PS/a small amount of UHMW-PS blends Rheol Acta 40:329-338 doi:10.1007/s003970100165

Mitomo H, Kaneda A, Quynh TM, Nagasawa N, Yoshii F (2005) Improvement of heat stability of poly(l-lactic acid) by radiation-induced crosslinking Polymer 46:4695-4703 doi:http://dx.doi.org/10.1016/j.polymer.2005.03.088

Naguib HE, Park CB, Panzer U, Reichelt N (2002) Strategies for achieving ultra low-density polypropylene foams Polym Eng Sci 42:1481-1492 doi:10.1002/pen.11045

Naguib HE, Park CB, Reichelt N (2004) Fundamental foaming mechanisms governing the volume expansion of extruded polypropylene foams J Appl Polym Sci 91:2661-2668 doi:10.1002/app.13448

Najafi N, Heuzey MC, Carreau PJ, Wood-Adams PM (2012) Control of thermal degradation of polylactide (PLA)-clay nanocomposites using chain extenders Polym Degrad Stabil 97:554-565 doi:http://dx.doi.org/10.1016/j.polymdegradstab.2012.01.016

Nofar M, Barzegari MR, Tabatabae iA, Keshtkar M, Park CB (2012) Effect of various additives (talc, nanoclay, and nanosilica) on extrusion foaming of pla through crystallization. Paper presented at the Annual Technical Conference - ANTEC,

Nofar M, Park CB (2014) Poly (lactic acid) Foaming: A Review Prog Polym Sci doi:http://dx.doi.org/10.1016/j.progpolymsci.2014.04.001

Nofar M, Tabatabaei A, Ameli A, Park CB (2013) Comparison of melting and crystallization behaviors of polylactide under high-pressure CO_2, N_2, and He Polymer 54:6471-6478 doi:http://dx.doi.org/10.1016/j.polymer.2013.09.044

Park CB, Baldwin DF, Suh NP (1995) Effect of the pressure drop rate on cell nucleation in continuous processing of microcellular polymers Polym Eng Sci 35:432-440 doi:10.1002/pen.760350509

Pilla S, Kim SG, Auer GK, Gong S, Park CB (2009) Microcellular extrusion-foaming of polylactide with chain-extender Polym Eng Sci 49:1653-1660 doi:10.1002/pen.21385

Pilla S, Kim SG, Auer GK, Gong S, Park CB (2010a) Microcellular extrusion foaming of poly(lactide)/poly(butylene adipate-co-terephthalate) blends Mater Sci Eng 30:255-262 doi:http://dx.doi.org/10.1016/j.msec.2009.10.010

Pilla S, Kramschuster A, Lee J, Clemons C, Gong S, Turng L-S (2010b) Microcellular processing of polylactide-"hyperbranched polyester-nanoclay composites J Mater Sci 45:2732-2746 doi:10.1007/s10853-010-4261-6

Robertson CG, Roland CM, Puskas JE (2002) Nonlinear rheology of hyperbranched polyisobutylene J Rheol 46:307-320 doi:doi:http://dx.doi.org/10.1122/1.1428318

Seo J-H, Han J, Lee KS, Cha SW (2012) Combined Effects of Chemical and Microcellular Foaming on Foaming Characteristics of PLA (Poly Lactic Acid) in Injection Molding Process Polym Plast Tech Eng 51:455-460 doi:10.1080/03602559.2011.651239

So K (2012) Automotive giants turn to bioplastics Eur Plast News 39:31-32

Soppimath KS, Aminabhavi TM, Kulkarni AR, Rudzinski WE (2001) Biodegradable polymeric nanoparticles as drug delivery devices J Control Release 70:1-20 doi:http://dx.doi.org/10.1016/S0168-3659(00)00339-4

Spitael P, Macosko CW (2004) Strain hardening in polypropylenes and its role in extrusion foaming Polym Eng Sci 44:2090-2100 doi:10.1002/pen.20214

Taki K, Kitano D, Ohshima M (2011) Effect of Growing Crystalline Phase on Bubble Nucleation in Poly(L-Lactide)/CO2 Batch Foaming Ind Eng Chem Res 50:3247-3252 doi:10.1021/ie101637f

Theinsathid P, Chandrachai A, Keeratipibul S (2009) Managing Bioplastics Business Innovation in Start Up Phase 2009 4 doi:82-93

Tian J, Yu W, Zhou C (2006) The preparation and rheology characterization of long chain branching polypropylene Polymer 47:7962-7969 doi:http://dx.doi.org/10.1016/j.polymer.2006.09.042

Van Ruymbeke E, Keunings R, Bailly C (2005) Prediction of linear viscoelastic properties for polydisperse mixtures of entangled star and linear polymers: Modified tube-based model and comparison with experimental results J Non-Newtonian Fluid 128:7-22 doi:http://dx.doi.org/10.1016/j.jnnfm.2005.01.006

Wang J, Zhu W, Zhang H, Park CB (2012a) Continuous processing of low-density, microcellular poly(lactic acid) foams with controlled cell morphology and crystallinity Chem Eng Sci 75:390-399 doi:http://dx.doi.org/10.1016/j.ces.2012.02.051

Wang L, Jing X, Cheng H, Hu X, Yang L, Huang Y (2012b) Blends of Linear and Long-Chain Branched Poly(l-lactide)s with High Melt Strength and Fast Crystallization Rate Ind Eng Chem Res 51:10088-10099 doi:10.1021/ie300526u

Wang L, Jing X, Cheng H, Hu X, Yang L, Huang Y (2012c) Rheology and Crystallization of Long-Chain Branched Poly(l-lactide)s with Controlled Branch Length Ind Eng Chem Res 51:10731-10741 doi:10.1021/ie300524j

Wang L, Wan D, Qiu J, Tang T (2012d) Effects of long chain branches on the crystallization and foaming behaviors of polypropylene-g-poly(ethylene-co-1-butene) graft copolymers with well-defined molecular structures Polymer 53:4737-4757 doi:http://dx.doi.org/10.1016/j.polymer.2012.08.036

Wever DAZ, Picchioni F, Broekhuis AA (2013) Branched polyacrylamides: Synthesis and effect of molecular architecture on solution rheology Eur Polym J 49:3289-3301 doi:http://dx.doi.org/10.1016/j.eurpolymj.2013.06.036

Wong A, Guo Y, Park CB (2013) Fundamental mechanisms of cell nucleation in polypropylene foaming with supercritical carbon dioxide Effects of extensional stresses and crystals J Supercrit Fluids 79:142-151 doi:http://dx.doi.org/10.1016/j.supflu.2013.02.013

Wong A, Leung SN, Li GYG, Park CB (2007) Role of Processing Temperature in Polystyrene and Polycarbonate Foaming with Carbon Dioxide Ind Eng Chem Res 46:7107-7116 doi:10.1021/ie070551z

Wood-Adams PM, Dealy JM, deGroot AW, Redwine OD (2000) Effect of Molecular Structure on the Linear Viscoelastic Behavior of Polyethylene Macromolecules 33:7489-7499 doi:10.1021/ma991533z

You J, Lou L, Yu W, Zhou C (2013) The preparation and crystallization of long chain branching polylactide made by melt radicals reaction J Appl Polym Sci 129:1959-1970 doi:10.1002/app.38912

Zhu W, Zhou N, Wu H (2006) Multiplex shear stress-induced nucleation in dynamic microcellular foaming process Polym Eng Sci 46:1728-1738 doi:10.1002/pen.20651